Published in final edited form as:

Virology. 2018 May ; 518: 301–312. doi:10.1016/j.virol.2018.03.009.

Infection by Zika viruses requires the transmembrane protein AXL, endocytosis and low pH

Mirjana Persaud[a], **Alicia Martinez-Lopez**[a], **Cindy Buffone**[a], **Steven A. Porcelli**[a,b], **Felipe Diaz-Griffero**[a,*]

[a]Department of Microbiology and Immunology, Albert Einstein College of Medicine Bronx, NY 10461, USA

[b]Department of Medicine, Albert Einstein College of Medicine Bronx, NY 10461, USA

Abstract

The recent Zika virus (ZIKV) outbreak in Brazil has suggested associations of this virus infection with neurological disorders, including microcephaly in newborn infants and Guillian-Barré syndrome in adults. Previous reports have shown that AXL, a transmembrane receptor tyrosine kinase protein, is essential for ZIKV infection of mammalian cells, but this remains controversial. Here, we have assessed the involvement of AXL in the ability of ZIKV to infect mammalian cells, and also the requirement for endocytosis and acidic pH. We demonstrated that AXL is essential for ZIKV infection of human fibroblast cell line HT1080 as the targeted deletion of the gene for AXL in HT1080 cells made them no longer susceptible to ZIKV infection. Our results also showed that infection was prevented by lysosomotropic agents such as ammonium chloride, chloroquine and bafilomycin A1, which neutralize the normally acidic pH of endosomal compartments. Infection by ZIKV was also blocked by chlorpromazine, indicating a requirement for clathrin-mediated endocytosis. Taken together, our findings suggest that AXL most likely serves as an attachment factor for ZIKV on the cell surface, and that productive infection requires endocytosis and delivery of the virus to acidified intracellular compartments.

Keywords

ZIKA; Entry; Low-pH; Endocytosis; Clathrin

1. Introduction

The recent outbreak of Zika Virus (ZIKV) in Brazil has raised important public health issues, particularly due to possible associations with neurological disorders including microcephaly and Guillian-Barré syndrome. ZIKV is a mosquito-transmitted flavivirus closely related to Dengue virus (DENV), West Nile virus (WNV), and yellow fever virus (YFV). Although ZIKV is transmitted by mosquitos, recent reports indicate the potential for

*Correspondence to: Department of Microbiology and Immunology, Albert Einstein College of Medicine, 1301 Morris Park – Price Center 501, New York, NY 10461, USA. Felipe.Diaz-Griffero@einstein.yu.edu (F. Diaz-Griffero).

Appendix A. Supporting information

Supplementary data associated with this article can be found in the online version at http://dx.doi.org/10.1016/j.virol.2018.03.009.

male-to-female sexual transmission of the virus (Abushouk et al., 2016; Russell et al., 2017; Tang et al., 2016).

Similar to other flaviviruses, ZIKV contains a positive single-stranded genomic RNA encoding a polyprotein that is processed into three structural proteins [capsid (C), precursor of membrane (prM) and envelope (E)] and seven nonstructural proteins (NS1, NS2A, NS2B, NS3, NS4A, NS4B, NS5) (da Fonseca et al., 2017). ZIKV is a membrane enveloped virus that requires fusion of the viral membrane with host cell membranes in order to cause infection. Entry of ZIKV to target cells is coordinated by the E protein arrayed on the surface of the virion. Once the virion components have reached the cytoplasm, the NS proteins form a replication complex that synthesizes a negative-sense RNA, which subsequently serves as a template for the positive-sense RNA. The newly synthesized RNA is encapsidated, transported by the host secretory pathway, and released from the infected cell by exocytosis.

The entry of ZIKV into mammalian cells is poorly understood, although evidence suggests that the membrane protein AXL contributes to this process by serving an attachment factor at the cell surface (Hamel et al., 2015; Liu et al., 2016; Meertens et al., 2017; Savidis et al., 2016). However, entry of ZIKV has been observed in human and mouse cells that do not express AXL (Miner et al., 2016; Rausch et al., 2017; Wells et al., 2016), suggesting that there may be additional factors that can perform the required functions for ZIKV entry on at least some types of cells. A recent study suggested that the interaction of the ZIKV virion with AXL is mediated by the AXL ligand, Gas6 (Meertens et al., 2017), which has also been shown to be involved in the entry of other viruses (Meertens et al., 2012; Morizono and Chen, 2014). In this scenario, Gas6 interacts with both the surface-exposed phosphatidylserine on the ZIKV virion and AXL on the surface of the cell, bridging the interaction of the ZIKV virion with AXL. These findings open the possibility that other proteins with the ability to bind to phosphatidylserine are contributing to the entry of ZIKV into different cell types, including those that do not express AXL.

The current study was carried out to further explore the role of AXL in ZIKV entry into cells, and also to investigate the steps involved in infection by ZIKV after its interaction with the host cell membrane. Our results provided further support for AXL as a component of ZIKV entry, and also showed an essential requirement for endocytosis and acidification of intracellular compartments in the infection of mammalian cells by ZIKV.

2. Results

2.1. Detection methods to monitor ZIKV infection

To detect ZIKV infection, we used two different infection assays based on either ZIKV-reporter viral particles (ZIKV-RVPs) that express GFP as a reporter of infection, or infection of the wild type ZIKV strain from Uganda MR766. In the latter case, infection was measured by detecting expression of the ZIKV envelope on infected cells using the antibody 4G2 by flow cytometry in fixed/permeabilized cells (Enfissi et al., 2016).

To produce ZIKV-reporter viral particles, we took advantage of the West Nile virus (WNV) replicon GZ (Mukherjee et al., 2014), which encodes all non-structural proteins of this virus (Fig. 1A). The GZ replicon also encodes a GFP gene, inserted in between the capsid and the envelope protein consequently truncating both proteins (Fig. 1A). To generate ZIKV-reporter viral particles, we transfected 5 μg of the WNV replicon GZ together with 1 μg of the codon-optimized gene expressing the capsid (C), precursor of membrane (prM) and envelope (E) proteins of the ZIKV strain KU312312, which is the Suriname strain (Enfissi et al., 2016). We titered the ZIKV-RVP in African green monkey kidney (Vero) cells by limiting dilution analysis, measuring the percentage of GFP-positive cells to allow calculation of the viral titer.

To test this reporter assay, we challenged human microglial cells (CHME-3), human fibroblasts (HT-1080), Vero, and dog epithelial cells (Cf2Th) using ZIKV-RVP at an MOI of 1. As shown in Fig. 1B, infection was determined by measuring the percentage of GFP-positive cells. Although all four tested cell lines were infected by the ZIKV-RVP, Vero and Cf2Th cells were more susceptible to infection. Next we tested whether the entry of ZIKV-RVP could be blocked by specific antibodies against the envelope protein of ZIKV. We challenged Cf2Th cells using ZIKV-RVP at an MOI of 0.2 in the presence of increasing concentration of the indicated specific antibodies against the ZIKV envelope, and determined the percentage of GFP positive cells by flow cytometry 48 h post-infection. As shown in Fig. 1C, antibodies Z54 and Z67 potently neutralized the cellular entry of ZIKV-RVP, which is in agreement with previous results showing that these antibodies neutralize different ZIKV replication-competent strains (Zhao et al., 2016). By contrast, antibodies Z48 and Z64 poorly neutralized the entry of ZIKV-RVP, which was also consistent with previous findings (Zhao et al., 2016). As a control, we used the non-neutralizing, envelope-specific antibody 4G2 (Fig. 1C). These experiments provided support for the view that ZIKV-RVP was a reliable tool that faithfully replicates features of ZIKV entry into cells.

To detect replication of natural ZIKV, we used the ZIKV strain MR766 (ZIKV-MR766) to infect Vero cells followed by staining with monoclonal antibody 4G2 to quantitate infected cells (Fig. 2A), as previously described (Hamel et al., 2015). As shown in Fig. 2B, infected Vero cells were readily detected at 48 h post exposure to ZIKV when compared to the isotype matched control or samples stained with the secondary antibodies only. This assay was further validated by challenging Vero cells using a range of infectious doses of ZIKV-MR766 (Fig. 2C). Altogether, these results validated two different systems for the study of ZIKV entry and infection in our studies.

2.2. The role of AXL in ZIKV infection

The requirement for expression of AXL for infection by ZIKV was assessed using AXL deficient cell lines generated using the CRISPR/Cas9 system. Because fibroblasts are infected by Zika virus (Hamel et al., 2015; Hou et al., 2017), we decided to use as a model the cell line HT1080, which is composed of malignant fibroblasts. To investigate whether AXL plays a role in the entry of ZIKV into human cells, we used wild type and AXL knockout variants of the cell line HT1080. We obtained HT1080 clones with deletions and insertions in the *axl* gene that resulted in change of amino acid sequence and early

termination of the protein (Fig. 3A). As shown in Fig. 3B, clones 3-II and 1-IV, derived from HT1080 after targeted CRISPR/Cas9 deletion of the *axl* gene, did not express AXL in the cell surface as detected by a flow cytometry using anti-AXL antibodies. As a control, we used clone 1-F, which was isolated from cultures that were subjected to the same knockout procedure but did not lose expression of human AXL. To test the infectivity of these cell lines, we challenged them using increasing MOIs of the ZIKV strain MR766 and measured infection by flow cytometry using anti-4G2 antibodies 24 h post-infection. As shown in Fig. 3C, human HT1080 cells knockout for the expression of AXL (clones 3-II and 1-IV) were not infected by ZIKV when compared to the wild type parent HT1080 line or clone 1-F (Fig. 3C). Next, we sought to rescue ZIKV infection of HT1080 AXL KO clones by re-introducing the human AXL (hAXL) protein. To this end, using a lentiviral vector we expressed the hAXL protein in the HT1080 AXL KO clones (Fig. 3D). As expected, expression of hAXL in HT1080 AXL KO clones rescued the infection by ZIKVs (Fig. 3D). Overall, these results indicated that the AXL receptor was essential for the ability of ZIKV to infect human HT1080 cells, and are consistent with the notion that AXL is a relevant human receptor for ZIKV.

2.3. Infection of different cell types by ZIKV

In this section we sought to correlate cell surface expression of AXL with susceptibility to ZIKV infection. For this purpose, we first measured cell surface expression of AXL in HT1080, HEK293T, CHME and Vero cells. As shown in Fig. 4A, HT1080, CHME and Vero cells express similar surface levels of the AXL protein. By contrast, HEK293T cells did not show surface expression of AXL(Fig. 4A). Next we compared the ability of these cell lines to be infected by ZIKVs using increasing MOIs (Fig. 4B). As shown in Fig. 4B, CHME3 cells were highly susceptible to ZIKV infection, as previously shown (Meertens et al., 2017). In contrast, HEK293T cells were poorly susceptible to ZIKV infection, although the use of relatively high MOIs of 5 and 10 resulted in detectable levels of infection (Fig. 4B). Direct comparisons with HT1080 and Vero cells using a range of MOIs showed a clear hierarchy of susceptibility, with CHME3 most susceptible and HEK293T least susceptible to ZIKV infection. These experiments correlated expression of AXL with susceptibility to ZIKV infection.

2.4. Lysosomotropic agents block the entry of ZIKV

To evaluate the requirement for a low-pH compartment in ZIKV entry, we used lysosomotropic agents that block the acidification of endocytic vesicles, (Diaz-Griffero et al., 2002). We initially tested the effect of ammonium chloride in the infection of VERO and Cf2Th cells by ZIKV-RVP and ZIKV-MR766. As shown in Fig. 5A, the use of increasing concentrations of ammonium chloride potently blocked infection by ZIKV-RVP and ZIKV-MR776 viruses. As a control, we performed similar experiments using HIV-1 viruses pseudotyped with the pH-dependent envelope of the vesicular stomatitis virus (VSV-G). Similar results were observed with chloroquine, a lysosomotropic weak base that increases the endosomal pH (Fig. 5B). To prevent acidification by a different mechanism we used Bafilomycin A1 (Fig. 5C), which is a specific blocker of the v-type H^+-ATPase (Bowman et al., 1988). As a control, cell viability was determined in the presence of all lysosomotropic agents by measuring reduction of the tetrazolium dye MTT [3-(4,5-dimethylthiazol-2-

yl)-2,5-diphenyltetrazolium bromide] to its insoluble formazan (Fig. S1). These results showed that ZIKV entry required a low-pH compartment to develop productive infection, and revealed that ZIKV infection requires endocytosis.

2.5. Kinetics of ZIKV entry

The fact that ZIKV requires low pH for infection suggested that endocytic pathways are important for its ability to infect target cells. To evaluate the time required for ZIKV to travel from the cell surface to the fusion compartment and fuse with cellular membranes, we measured the kinetics of ZIKV entry. ZIKV-RVPs were pre-bound to cells at 4 °C for 1 h, and infection was then initiated by shifting the temperature to 37 °C. As shown in Fig. 6A, we added 20 mM ammonium chloride at the indicated times post-infection to prevent fusion. Infection was measured as indicated 48 h post-infection. Our analysis revealed that ZIKV-RVP viruses exhibit a $t_{1/2}$ of ~2–4 h for viral endocytosis and fusion with cellular membranes in Vero and HT1080 cells.

2.6. Stability of ZIKV in endocytic compartments

Our results strongly suggested that ZIKV requires endocytosis for viral entry. This evidence raises the question of how stable these viral particles are in endocytic compartments such as endosomes and lysosomes. To answer this question, we measured the stability of ZIKV-MR766 viruses in endocytic vesicles. To this end, we pre-bound ZIKV-MR766 viruses in the presence of 20 mM ammonium chloride for 1 h at 4 °C. Subsequently, infection was initiated by shifting the temperature to 37 °C and then removing ammonium chloride at the indicated times post-infection (Fig. 6B). Infection was measured 48 h post-infection, which revealed that the half-life of ZIKV-MR766 in the endocytic compartment (stability) was approximately 2–4 h.

2.7. Role of clathrin-mediated uptake in ZIKV entry

To test whether clathrin-mediated uptake is involved in the entry of ZIKV, we took advantage of the clathrin inhibitor chlorpromazine, which is a cationic amphiphilic drug that disrupts clathrin-mediated uptake by relocating clathrin and adaptor protein-2 complexes from the cell surface (Pho et al., 2000; Wang et al., 1993). As shown in Fig. 7, entry of ZIKV-RVP and ZIKV-MR766 was inhibited by increasing concentrations of chrlopromazine in Vero or Cf2Th cells. As a positive control, we confirmed the ability of HIV-1 viruses pseudotypes with VSV-G to be inhibited by chlorpromazine. Cell viability was determined in the presence of chlorpromazine by measuring reduction of the tetrazolium dye MTT to formazan(Fig. S1).

3. Discussion

Using fibroblasts that were deficient in AXL expression, we demonstrated involvement of this protein in the ability of ZIKV to infect human cells. Our findings using HT1080 fibroblasts with deletion of AXL were consistent with other reports showing that knock outs of AXL expression in microgial cells (CHME3), glioblastoma cells (U87), or epithelial cells (HeLa) prevented the infection by ZIKVs (Chan et al., 2016; Coelho et al., 2017; Hastings et al., 2017; Meertens et al., 2017; Retallack et al., 2016; Savidis et al., 2016; Vicenti et al.,

2018). Interestingly, with the exception of Hastings and colleagues whom rescue ZIKA infection of HeLa AXL KO cells by expressing the mouse AXL protein, none of these reports have rescued the infection by re-introducing the human AXL protein in KO cells. To remediate this, we rescued ZIKA infection in HT1080 cells knockout for the expression of AXL by expressing the human AXL protein(Fig. 3D). Altogether, these experiments suggested an essential role for AXL during ZIKV infection. By contrast, the literature also shows examples in which ablation of AXL expression does not affect ZIKV infection. For example, ablation of AXL in human neuroprogenitor cells (Wells et al., 2016), human placental cells (Rausch et al., 2017), or in mice (Govero et al., 2016; Miner et al., 2016), did not affect ZIKV infection. Overall these experiments suggested that ZIKVs might be using different attachment factors to enter cells. One possibility is that ZIKVs utilize different attachment factors such as AXL and a separate receptor that is involved in the fusion. It is important to point out that AXL binds to the Gas6 protein, which interacts with the phosphatidylserine in the viral membrane (Meertens et al., 2017), suggesting that AXL is an attachment factor. This raises the question whether the envelope protein of ZIKV, which contains the fusion machinery, interacts or not with a cellular protein that might be the receptor. Although in the case of flaviviruses is believed that the envelope does not require to interact with a cellular receptor for fusion (Stiasny and Heinz, 2006), the aforementioned controversy regarding ZIKV entry might suggest the existence of other attachment factors or receptors that may interact with the envelope protein. Future experiments in our laboratory will pursue whether the ZIKV envelope protein interacts with other membrane receptors.

Using our infection assays, we also explored whether low-pH compartments were required for the entry of ZIKVs in mammalian cells. Lysosomotropic agents such as ammonium chloride, chloroquine and Bafilomycin A1, strongly inhibited the ability of ZIKVs to enter mammalian cells. Our results are in agreement with the findings of others suggesting that ammonium chloride and chloroquine blocks ZIKVs infection (Delvecchio et al., 2016; Li et al., 2017; Rausch et al., 2017). These experiments suggested that ZIKVs infection require a low pH compartment and that ZIKVs are endocytosed before the viral membrane fuses with the cellular membrane. Our findings are in agreement with the notion that the entry of other flaviviruses such as dengue, Tick-borne encephalitis and West Nile viruses demonstrating a requirement for low pH during entry (Gollins and Porterfield, 1986; Randolph and Stollar, 1990; Smit et al., 2011; Vorovitch et al., 1991). Our results suggested that ZIKV entry requires low pH for fusion and involves endocytosis, which has been shown to be important for cell entry of flaviviruses (Pierson and Kielian, 2013).

To determine the kinetics of entry of ZIKV into mammalian cells, we prebound viruses to the surface of cells and stopped infection by adding a lyssomotropic agent at the indicated times. This allowed us to calculate a $t_{1/2}$ of 2–4 h for ZIKVs to reach the fusion compartment from the cell surface, illustrating the time required by the particle to reach the fusion compartment. Cortese and colleagues have shown that the virus requires a total time of 3 h to reach the fusion compartment in the human hepatic cell line Huh7 (Cortese et al., 2017). One possibility is that the differences may be due to that we are comparing different cell lines.

After contacting the cell surface, viruses that require low pH for infection, undergo receptor-mediated endocytosis. Here we tested whether clathrin mediated endocytosis is important for ZIKVs entry. Interestingly, the use of chlorpromazine, which is a cationic amphiphilic drug that disrupts clathrin-mediated uptake by relocating clathrin and adaptor protein 2 complexes from the cell surface (Pho et al., 2000; Wang et al., 1993), completely blocks the infection by ZIKVs. These experiments suggested that clathrin-mediated endocytosis is involved in the ability of ZIKVs to enter mammalian cells, which is in agreement with similar findings for ZIKVs and other flaviviruses such as dengue (Meertens et al., 2017; Pierson and Kielian, 2013; van der Schaar et al., 2008). In summary our work suggested that ZIKVs require AXL, low pH and endocytosis for infection of mammalian cells.

4. Materials and methods

4.1. Cells, viruses and compounds

Vero cells (ATCC CCL-81), HT-1080 cells (ATCC CCL-121) CHME3 cells (human microglia cell), HEK293T cells (ATCC CRL-3216) were grown at 37 °C in 5% CO_2 in Dulbecco's modified Eagle's medium (DMEM) supplemented with 10% fetal calf serum, 100 IU/mL of penicillin and 100 μg/mL of streptomycin. Cells were seeded in 24-well plates (50,000 cells/well) 24 h prior to infection with ZIKV at the multiplicities of infection (MOI) indicated in each experiment.

ZIKV strain MR766(a gift from Dr. Paul Bates), which is the first described ZIKV strain that was isolated in the Zika Forest of Uganda in 1947 (DICK et al., 1952), was produced and expanded in Vero cells. Vero cells were seeded in 10 cm plates 24 h prior to ZIKV infection. Cells were infected with ZIKV at an MOI 10 in DMEM supplemented media with 10% FCS and additives as above plus 25 mM HEPES for 3 h. An additional 5 mL more of the same media was subsequently added. The cultures were maintained for 72 h at 37 °C, after which the supernatant was collected and centrifuged for 10 min at 3000 × *g*. ZIKV was stores in aliquots at − 80 C until use.

A Zika virus reporter viral particle (ZIKV-RVP) was produced by cotransfection of two plasmids, designated ZIKV CPrME and WNV-NSGFP. The ZIKV CPrME construct encoded the ZIKV structural genes capsid (C), signal sequence, pro-membrane protein (PrM) and envelope protein (E) from the ZIKV strain. Sequences used were from the Suriname strain KU312312, which is the strain involved in a recent Brazilian outbreak of infection (Enfissi et al., 2016). The ZIKV genes were codon optimized for mammalian cells. The WNV-NS-GFP encoded the nonstructural genes of West Nile Virus (WNV) and a GFP reporter (Mukherjee et al., 2014). All but the first 20 amino acids of the capsid and the last 28 amino acids of envelope of WNV genome were been replaced with GFP. To generate viral particles, HEK293T cells were cotransfected with 1 μg of ZIKV CPrME and 5 μg of WNV-NS-GFP using polyethylimine transfection reagent at 1 mg/mL in serum free DMEM. Twenty-four hours post-transfection, the media was replaced with fresh DMEM and left for an additional 24 h. Supernatant containing infectious virus was collected, and centrifuged at 3000 × *g* for 10 min to remove cellular debris. Virus stocks were stored at − 80 °C and were thawed at 37 C immediately before use.

HIV-1-VSV-G viruses were produced by transfecting 1 μg HDM (HIV-1 gag-pol of HIV-1 NL4–3), 1 μg tat, 1 μg rev, 5 μg LTR-GFP-LTR and 2 μg VSV-G. Viruses were collected 48 h post-transfection and stored at − 80 °C, as previously described (Lienlaf et al., 2011).

Chloroquine (ACROS 455240250) and Ammonium Chloride (SIGMA A-0171) were dissolved in water to yield a 1 M stock. Bafilomycin A1 (Cayman Chemical Company, 11038–500) and Chlorpromazine (Santa Cruz SC-202537) were dissolved in DMSO to yield 1 mM and 50 mM stocks, respectively.

4.2. Detection of infection by ZIKV strain MR766

5×10^4 cells per well were challenged by ZIKV strain MR766 at different MOIs for 24 or 48 h. Subsequently, cells were detached using EDTA (5 mM) in PBS, collected by centrifugation and fixed with 1.5% paraformaldehyde in PBS for 15 min. The cells were then suspended in 0.1 M glycine for 10 min to quench the paraformaldehyde, and then washed with PBS. Cells were blocked for 30 min using 1 × Perm/Wash solution (BD Bioscience 51–2091KZ) in PBS and then incubated for 45 min in the same solution with anti-ZIKV E protein specific mAb 4G2 [gift of Dr. A. Brass (Savidis et al., 2016)], used as purified antibody. As a control, an isotype-matched non-binding mouse IgG1 mAb (Invitrogen Ms IgG1) was used at approximately the same concentration on replicate samples. Afterwards, cells were washed 3 times with 1 × Perm Wash buffer and incubated with goat anti-mouse Alexa488 labeled antibodies (Invitrogen, diluted 1:2000). Positive cells (ZIKV infected) were detected using a FACSCalibur flow cytometer (Becton Dickinson). This method for quantitating infection was also used for titration of ZIKV MR766 stocks on Vero cells. The titer was determined as the highest dilution of virus at which infected cells were detected significantly above the background of control antibody stained samples.

4.3. Detection of infection and antibody neutralization using ZIKV-RVP

5×10^4 cells per well were challenged by ZIKV-RVP at different MOIs for 24 or 48 h. Subsequently, cells were detached with 300 μl of 0.25% trypsin, and GFP-positive cells were measured using a FACSCalibur flow cytometer (Becton Dickinson). This method was also used to titrate ZIKV-RVP on Vero cells, except that GFP positive cells were quantitated at 72 h by fluorescence microscopy. For neutralization studies, antibodies against the ZIKV envelope protein [Z54, Z67, Z48 and Z64; all provided by Dr. M. Diamond (Zhao et al., 2016)] and the pan Flavivirus 4G2 monoclonal antibody were used at a range of concentrations and incubated together with ZIKV-RVP (MOI 0.2) for 1 h at 37 °C. Subsequently, the antibody-ZIKV-RVP mixtures were used to infect cells. Forty eight hours post-challenge, infection of cells was measured by determining the percentage of GFP-positive cells using a flow cytometer. The titer was calculated considering the highest dilution in which infected cells were detected.

4.4. Detection of AXL expression

HT1080 cells were seeded in 6 well plates at 2.5×10^5 per well, and then fixed and stained using goat polyclonal anti-human AXL antibodies (Bio-techne AF154) at 1 μg/mL. Secondary staining was performed using donkey anti-goat Alexa Fluor 488 antibodies (1:2000) and then analyzed by flow cytometry.

4.5. Generation of AXL knock out cell lines

AXL knockout (KO) cell lines were generated by using the clustered regularly interspaced short palindromic repeat (CRISPR)-Cas9 gene system (Edit-R CRISPR-Cas9 gene engineering with SMARTCas9 nucleases; GE Healthcare). The CRISPR genomic guide RNA sequences for human AXL in human fibrosarcoma HT-1080 cells were designed to target exon 4 and 7 (Guide 1: ACGAUGGGAUGGGCAUCC; Guide 2: CGGAUGCUUGCGAGGUGA;Guide 3: UCUCCACAGGAAGCCAGU). The guide RNA constructs together with hCMV-mKate2-Cas9 expression plasmid were cotransfected into HT-1080 cells. At 48 h after transfection, RFP-positive cells were single-cell sorted by using the FACSAria system (BD Biosciences, Franklin Lakes, NJ, USA). Clonal HT-1080colonies were expanded and characterized for the loss of AXL protein expression by FACS analysis using anti-AXL antibodies (Bio-techne AF154).

4.6. Statistical analysis and calculation of t1/2

To compare the effects of each treatment in relation to its control, all data was analyzed using two-tailed Student's t-test. Differences were considered statistically significant at $P < 0.05$ (*), $P < 0.01$ (**), $P < 0.001$ (***) or non-significant (ns).

The t1/2 for viral endocytosis and stability is an approximation derived from the experimental data as the necessary time required to achieve half of the infection using three independent data sets.

Supplementary Material

Refer to Web version on PubMed Central for supplementary material.

Acknowledgements

We thank Theodore Pierson and Kim Dowd for providing the WNV reporter plasmids, Michael Diamond for providing antibodies against the ZIKA envelope, Abraham Brass for providing the hybridoma cell line to produce 4G2, and Paul Bates for providing the ZIKA strain MR766.

References

Abushouk AI, Negida A, Ahmed H, 2016 An updated review of Zika virus. J. Clin. Virol 84, 53–58. 10.1016/j.jcv.2016.09.012. [PubMed: 27721110]

Bowman EJ, Siebers A, Altendorf K, 1988 Bafilomycins: a class of inhibitors of membrane ATPases from microorganisms, animal cells, and plant cells. Proc. Natl. Acad. Sci. USA 85, 7972–7976. [PubMed: 2973058]

Chan JF-W, Yip CC-Y, Tsang JO-L, Tee K-M, Cai J-P, Chik KK-H, Zhu Z, Chan CC-S, Choi GK-Y, Sridhar S, Zhang AJ, Lu G, Chiu K, Lo AC-Y, Tsao S-W, Kok K-H, Jin D-Y, Chan K-H, Yuen K-Y, 2016 Differential cell line susceptibility to the emerging Zika virus: implications for disease pathogenesis, non-vector-borne human transmission and animal reservoirs. Emerg. Microbes Infect 5, e93 10.1038/emi.2016.99. [PubMed: 27553173]

Coelho SVA, Neris RLS, Papa MP, Schnellrath LC, Meuren LM, Tschoeke DA, Leomil L, Verçoza BRF, Miranda M, Thompson FL, Da Poian AT, Souza TML, Carneiro FA, Damaso CR, Assunção-Miranda I, de Arruda LB, 2017 Development of standard methods for Zika virus propagation, titration, and purification. J. Virol. Methods 246, 65–74. 10.1016/j.jviromet.2017.04.011. [PubMed: 28445704]

Cortese M, Goellner S, Acosta EG, Neufeldt CJ, Oleksiuk O, Lampe M, Haselmann U, Funaya C, Schieber N, Ronchi P, Schorb M, Pruunsild P, Schwab Y, Chatel-Chaix L, Ruggieri A, Bartenschlager R, 2017 Ultrastructural characterization of zika virus replication factories. Cell Rep 18, 2113–2123. 10.1016/j.celrep.2017.02.014. [PubMed: 28249158]

da Fonseca NJ, Lima Afonso MQ, Pedersolli NG, de Oliveira LC, Andrade DS, Bleicher L, 2017 Sequence, structure and function relationships in flaviviruses as assessed by evolutive aspects of its conserved non-structural protein domains. Biochem. Biophys. Res. Commun 10.1016/j.bbrc.2017.01.041.

Delvecchio R, Higa LM, Pezzuto P, Valadão AL, Garcez PP, Monteiro FL, Loiola EC, Dias AA, Silva FJM, Aliota MT, Caine EA, Osorio JE, Bellio M, O'Connor DH, Rehen S, de Aguiar RS, Savarino A, Campanati L, Tanuri A, 2016 Chloroquine, an endocytosis blocking agent, inhibits Zika virus infection in different cell models. Viruses 8 10.3390/v8120322.

Diaz-Griffero F, Hoschander SA, Brojatsch J, 2002 Endocytosis is a critical step in entry of subgroup B avian leukosis viruses. J. Virol 76, 12866–12876. [PubMed: 12438612]

Dick GWA, Kitchen SF, Haddow AJ, 1952 Zika virus. I. Isolations and serological specificity. Trans. R. Soc. Trop. Med. Hyg 46, 509–520. [PubMed: 12995440]

Enfissi A, Codrington J, Roosblad J, Kazanji M, Rousset D, 2016 Zika virus genome from the Americas. Lancet 387, 227–228. 10.1016/S0140-6736(16)00003-9. [PubMed: 26775124]

Gollins SW, Porterfield JS, 1986 pH-dependent fusion between the flavivirus West Nile and liposomal model membranes. J. Gen. Virol 67 (Pt 1), 157–166. 10.1099/0022-1317-67-1-157. [PubMed: 3944582]

Govero J, Esakky P, Scheaffer SM, Fernandez E, Drury A, Platt DJ, Gorman MJ, Richner JM, Caine EA, Salazar V, Moley KH, Diamond MS, 2016 Zika virus infection damages the testes in mice. Nature 540, 438–442. 10.1038/nature20556. [PubMed: 27798603]

Hamel R, Dejarnac O, Wichit S, Ekchariyawat P, Neyret A, Luplertlop N, Perera-Lecoin M, Surasombatpattana P, Talignani L, Thomas F, Cao-Lormeau V-M, Choumet V, Briant L, Desprès P, Amara A, Yssel H, Missé D, 2015 Biology of Zika virus infection in human skin cells. J. Virol 89, 8880–8896. 10.1128/JVI.00354-15. [PubMed: 26085147]

Hastings AK, Yockey LJ, Jagger BW, Hwang J, Uraki R, Gaitsch HF, Parnell LA, Cao B, Mysorekar IU, Rothlin CV, Fikrig E, Diamond MS, Iwasaki A, 2017 TAM receptors are not required for Zika virus infection in mice. Cell Rep 19, 558–568. 10.1016/j.celrep.2017.03.058. [PubMed: 28423319]

Hou W, Armstrong N, Obwolo LA, Thomas M, Pang X, Jones KS, Tang Q, 2017 Determination of the cell permissiveness spectrum, mode of RNA replication, and RNA-protein interaction of Zika virus. BMC Infect. Dis 17, 239 10.1186/s12879-017-2338-4. [PubMed: 28359304]

Li C, Zhu X, Ji X, Quanquin N, Deng Y-Q, Tian M, Aliyari R, Zuo X, Yuan L, Afridi SK, Li X-F, Jung JU, Nielsen-Saines K, Qin FX-F, Qin C-F, Xu Z, Cheng G, 2017 Chloroquine, a FDA-approved drug, prevents Zika virus infection and its associated congenital microcephaly in mice. EBioMedicine 24, 189–194. 10.1016/j.ebiom.2017.09.034. [PubMed: 29033372]

Lienlaf M, Hayashi F, Di Nunzio F, Tochio N, Kigawa T, Yokoyama S, Diaz-Griffero F, 2011 Contribution of E3-ubiquitin ligase activity to HIV-1 restriction by TRIM5 rh: structure of the RING domain of TRIM5. J. Virol 85, 8725–8737. 10.1128/JVI.00497-11. [PubMed: 21734049]

Liu S, DeLalio LJ, Isakson BE, Wang TT, 2016 AXL-mediated productive infection of human endothelial cells by Zika virus. Circ. Res 119, 1183–1189. 10.1161/CIRCRESAHA.116.309866. [PubMed: 27650556]

Meertens L, Carnec X, Lecoin MP, Ramdasi R, Guivel-Benhassine F, Lew E, Lemke G, Schwartz O, Amara A, 2012 The TIM and TAM families of phosphatidylserine receptors mediate dengue virus entry. Cell Host Microbe 12, 544–557. 10.1016/j.chom.2012.08.009. [PubMed: 23084921]

Meertens L, Labeau A, Dejarnac O, Cipriani S, Sinigaglia L, Bonnet-Madin L, Le Charpentier T, Hafirassou ML, Zamborlini A, Cao-Lormeau V-M, Coulpier M, Missé D, Jouvenet N, Tabibiazar R, Gressens P, Schwartz O, Amara A, 2017 Axl mediates ZIKA virus entry in human glial cells and modulates innate immune responses. Cell Rep 18, 324–333. 10.1016/j.celrep.2016.12.045. [PubMed: 28076778]

Miner JJ, Sene A, Richner JM, Smith AM, Santeford A, Ban N, Weger-Lucarelli J, Manzella F, Rückert C, Govero J, Noguchi KK, Ebel GD, Diamond MS, Apte RS, 2016 Zika virus infection in

mice causes panuveitis with shedding of virus in tears. Cell Rep 16, 3208–3218. 10.1016/j.celrep.2016.08.079. [PubMed: 27612415]

Morizono K, Chen ISY, 2014 Role of phosphatidylserine receptors in enveloped virus infection. J. Virol 88, 4275–4290. 10.1128/JVI.03287-13. [PubMed: 24478428]

Mukherjee S, Pierson TC, Dowd KA, 2014 Pseudo-infectious reporter virus particles for measuring antibody-mediated neutralization and enhancement of dengue virus infection. Methods Mol. Biol 1138, 75–97. 10.1007/978-1-4939-0348-1_6. [PubMed: 24696332]

Pho MT, Ashok A, Atwood WJ, 2000 JC virus enters human glial cells by clathrin-dependent receptor-mediated endocytosis. J. Virol 74, 2288–2292. [PubMed: 10666259]

Pierson TC, Kielian M, 2013 Flaviviruses: braking the entering. Curr. Opin. Virol 3,3–12. 10.1016/j.coviro.2012.12.001. [PubMed: 23352692]

Randolph VB, Stollar V, 1990 Low pH-induced cell fusion in flavivirus-infected Aedes albopictus cell cultures. J. Gen. Virol 71 (Pt 8), 1845–1850. 10.1099/0022-1317-71-8-1845. [PubMed: 2167941]

Rausch K, Hackett BA, Weinbren NL, Reeder SM, Sadovsky Y, Hunter CA, Schultz DC, Coyne CB, Cherry S, 2017 Screening bioactives reveals nanchangmycin as a broad spectrum antiviral active against Zika virus. Cell Rep 18, 804–815. 10.1016/j.celrep.2016.12.068. [PubMed: 28099856]

Retallack H, Di Lullo E, Arias C, Knopp KA, Laurie MT, Sandoval-Espinosa C, Mancia Leon WR, Krencik R, Ullian EM, Spatazza J, Pollen AA, Mandel-Brehm C, Nowakowski TJ, Kriegstein AR, DeRisi JL, 2016 Zika virus cell tropism in the developing human brain and inhibition by azithromycin. Proc. Natl. Acad. Sci 113, 14408–14413. 10.1073/pnas.1618029113. [PubMed: 27911847]

Russell K, Hills SL, Oster AM, Porse CC, Danyluk G, Cone M, Brooks R, Scotland S, Schiffman E, Fredette C, White JL, Ellingson K, Hubbard A, Cohn A, Fischer M, Mead P, Powers AM, Brooks JT, 2017 Male-to-female sexual transmission of Zika virus-United States, January-April 2016. Clin. Infect. Dis 64, 211–213. 10.1093/cid/ciw692. [PubMed: 27986688]

Savidis G, McDougall WM, Meraner P, Perreira JM, Portmann JM, Trincucci G, John SP, Aker AM, Renzette N, Robbins DR, Guo Z, Green S, Kowalik TF, Brass AL, 2016 Identification of Zika virus and dengue virus dependency factors using functional genomics. Cell Rep 16, 232–246. 10.1016/j.celrep.2016.06.028. [PubMed: 27342126]

Smit JM, Moesker B, Rodenhuis-Zybert I, Wilschut J, 2011 Flavivirus cell entry and membrane fusion. Viruses 3, 160–171. 10.3390/v3020160. [PubMed: 22049308]

Stiasny K, Heinz FX, 2006 Flavivirus membrane fusion. J. Gen. Virol 87, 2755–2766. 10.1099/vir.0.82210-0. [PubMed: 16963734]

Tang WW, Young MP, Mamidi A, Regla-Nava JA, Kim K, Shresta S, 2016 A Mouse model of Zika virus sexual transmission and vaginal viral replication. Cell Rep 17, 3091–3098. 10.1016/j.celrep.2016.11.070. [PubMed: 28009279]

van der Schaar HM, Rust MJ, Chen C, van der Ende-Metselaar H, Wilschut J, Zhuang X, Smit JM, 2008 Dissecting the cell entry pathway of dengue virus by single-particle tracking in living cells. PLoS Pathog 4, e1000244 10.1371/journal.ppat.1000244. [PubMed: 19096510]

Vicenti I, Boccuto A, Giannini A, Dragoni F, Saladini F, Zazzi M, 2018 Comparative analysis of different cell systems for Zika virus (ZIKV) propagation and evaluation of anti-ZIKV compounds in vitro. Virus Res 244, 64–70. 10.1016/j.virusres.2017.11.003. [PubMed: 29113824]

Vorovitch MF, Timofeev AV, Atanadze SN, Tugizov SM, Kushch AA, Elbert LB, 1991 pH-dependent fusion of tick-borne encephalitis virus with artificial membranes. Arch. Virol 118, 133–138. [PubMed: 2048972]

Wang LH, Rothberg KG, Anderson RG, 1993 Mis-assembly of clathrin lattices on endosomes reveals a regulatory switch for coated pit formation. J. Cell Biol 123, 1107–1117. [PubMed: 8245121]

Wells MF, Salick MR, Wiskow O, Ho DJ, Worringer KA, Ihry RJ, Kommineni S, Bilican B, Klim JR, Hill EJ, Kane LT, Ye C, Kaykas A, Eggan K, 2016 Genetic ablation of AXL does not protect human neural progenitor cells and cerebral organoids from Zika virus infection. Cell Stem Cell 19, 703–708. 10.1016/j.stem.2016.11.011. [PubMed: 27912091]

Zhao H, Fernandez E, Dowd KA, Speer SD, Platt DJ, Gorman MJ, Govero J, Nelson CA, Pierson TC, Diamond MS, Fremont DH, 2016 Structural basis of Zika virus-specific antibody protection. Cell 166, 1016–1027. 10.1016/j.cell.2016.07.020. [PubMed: 27475895]

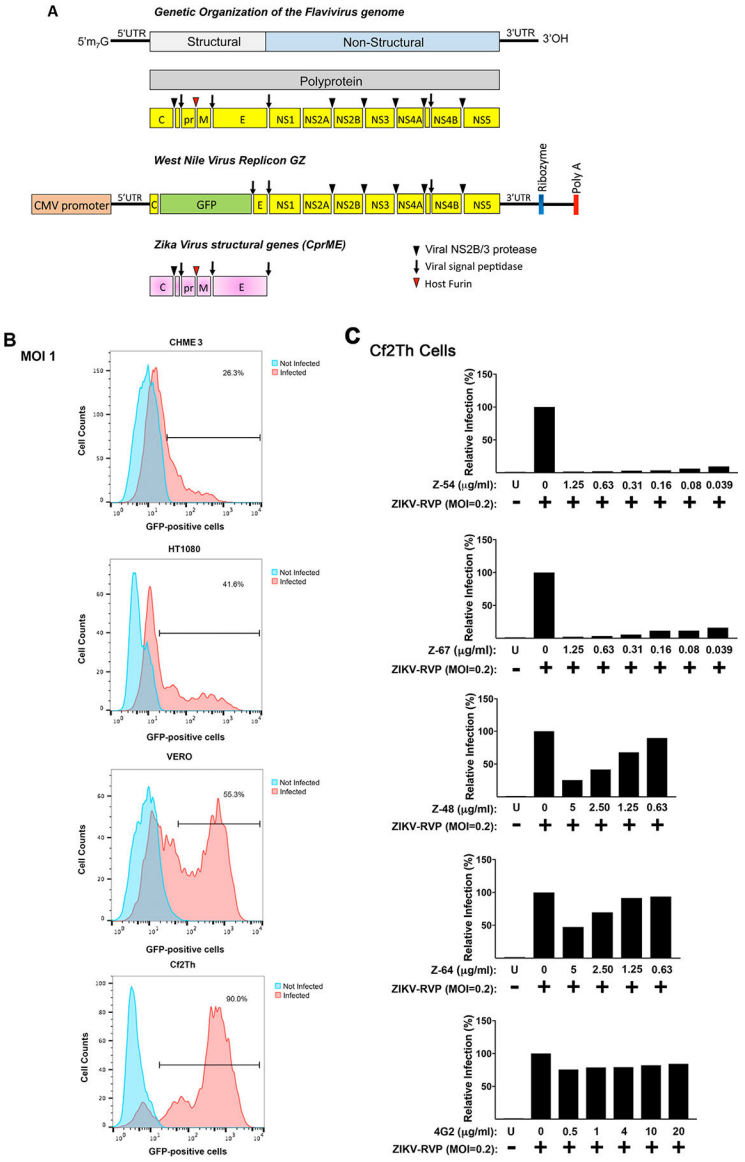

Fig. 1. Construction of ZIKV-reporter viral particles (ZIKV-RVPs).

(A) The genetic organization of the Flavivirus genome is shown. The Flaviviruses genome is translated into a single polyprotein that is proteolytically processed into the illustrated structural and non-structural proteins. The West Nile Virus replicon GFP and Zeocin (GZ) is shown, which is the genome of West Nile virus where the GFP protein has been inserted replacing part of the capsid (C), promembrane (prM) and part of the envelope (E). The Zika Virus structural gens are shown. To create ZIKV-RVPs, human HEK293T cells were transfected the 5 µg of the West Nile virus replicon GZ together with 1 µg of the Zika Virus structural genes. Supernatants containing ZIKV-RVPs were collected 48 h post transfection, and ZIKV-RVPs were tittered in Vero cells using serial dilutions. **(B)** ZIKV-RVPs infect human microglial CHME3, human fibroblasts HT1080, African green monkey fibroblast-like Vero, and dog Cf2Th cells. CHME3, HT1080, Vero and Cf2Th cells were challenges by ZIKV-RVPs at an MOI of 1. Forty-eight hours post-challenge infection was determined by

measuring the percentage of GFP-positive cells using a flow cytometer. Experiments were repeated 5 times and a representative experiment is shown. **(C)** Neutralizing antibodies against the envelope of ZIKV inhibit the infection by ZIKV-RVPs. To determine whether neutralizing antibodies against the envelope of ZIKV inhibit the infection by ZIKV-RVPs, we challenged Cf2Th cells using ZIKV-RVPs that were pre-incubated with the indicated antibody for an hour at 37 °C. Forty-eight hours post-challenge infection was determined by measuring the percentage of GFP-positive cells using a flow cytometer. Experiments were repeated three times and a representative neutralization curve for each antibody is shown.

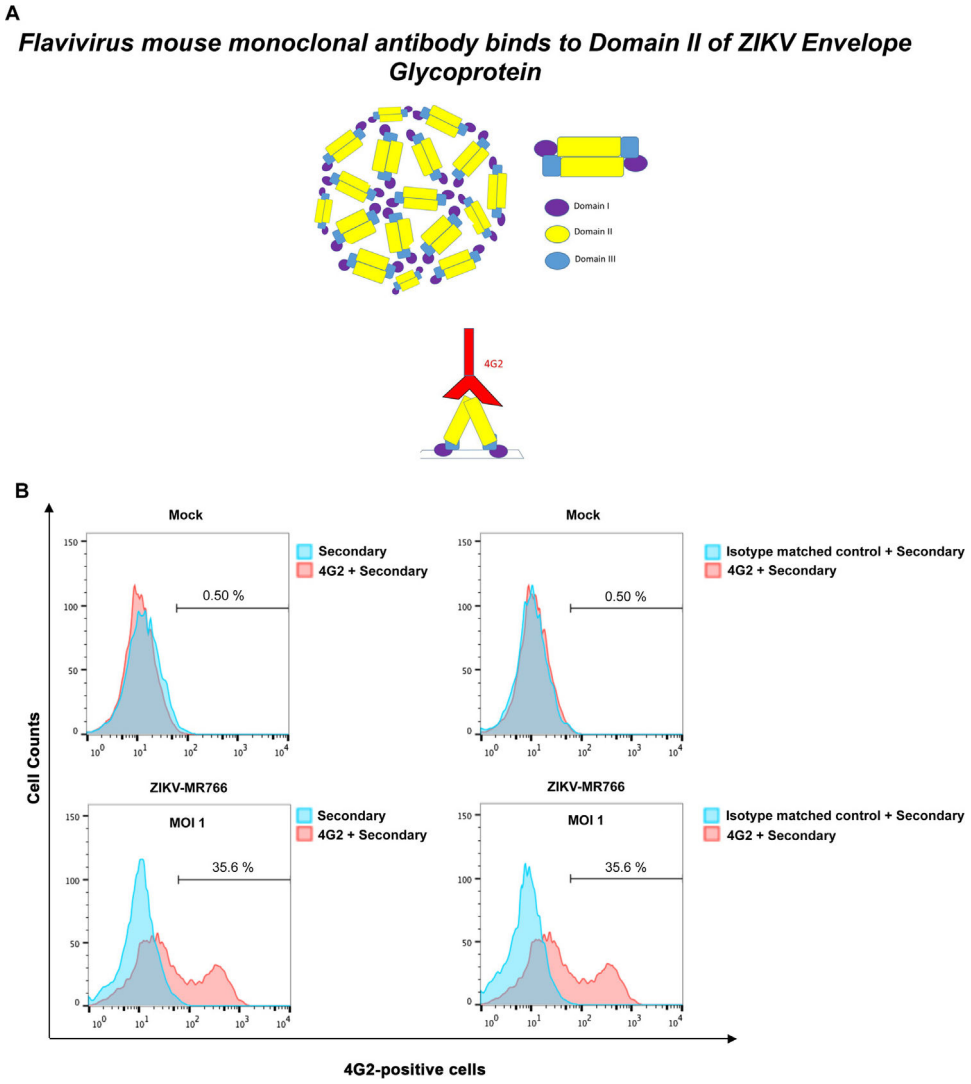

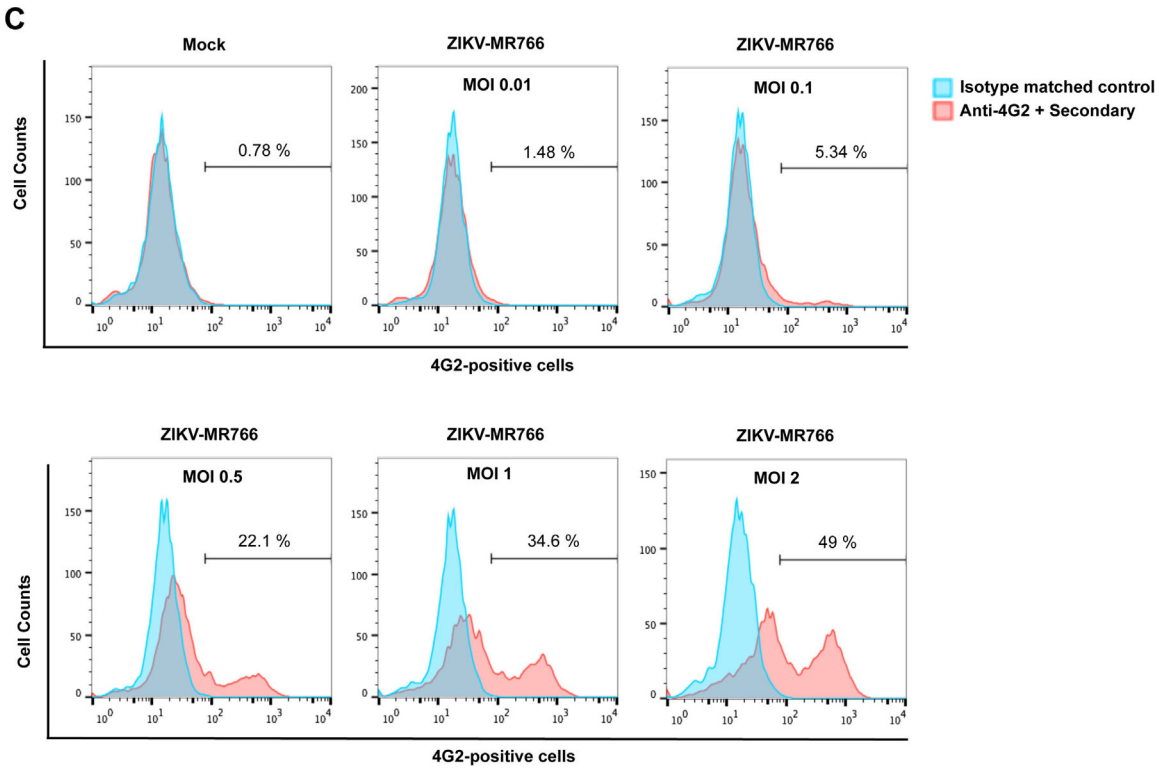

Fig. 2. Detection of wild type ZIKV infection using the anti-envelope monoclonal antibody 4G2.

(A) The domains I, II and III of the ZIKV envelope glycoprotein are depicted. The mouse monoclonal antibody 4G2 (red) binds to the fusion loop of Domain II. **(B)** The monoclonal antibody 4G2 recognizes ZIKV-infected Vero cells. Vero cells were challenged by ZIKV strain MR766 (ZIKV-MR766) at an MOI of 1 (lower panels). Twenty-four hours post-challenge cells were fixed/permeabilized, and infection was determined by staining cells using anti-ZIKA envelope antibodies 4G2. The percentage of infected cells was measured by counting the number of 4G2-positive cells using a flow cytometer. As a control, fixed/permeabilized infected cells were also stained using an isotype matched control antibody. We performed similar experiments using fixed/permeabilized mock infected cells. **(C)** Infection of Vero cells by ZIKA viruses at different MOIs. Vero cells were challenged by ZIKA-MR766 at increasing MOIs. The percentage of infected cells was measured by counting the number of 4G2-positive cells using a flow cytometer. Experiments were performed at least three times and a representative experiment is shown.

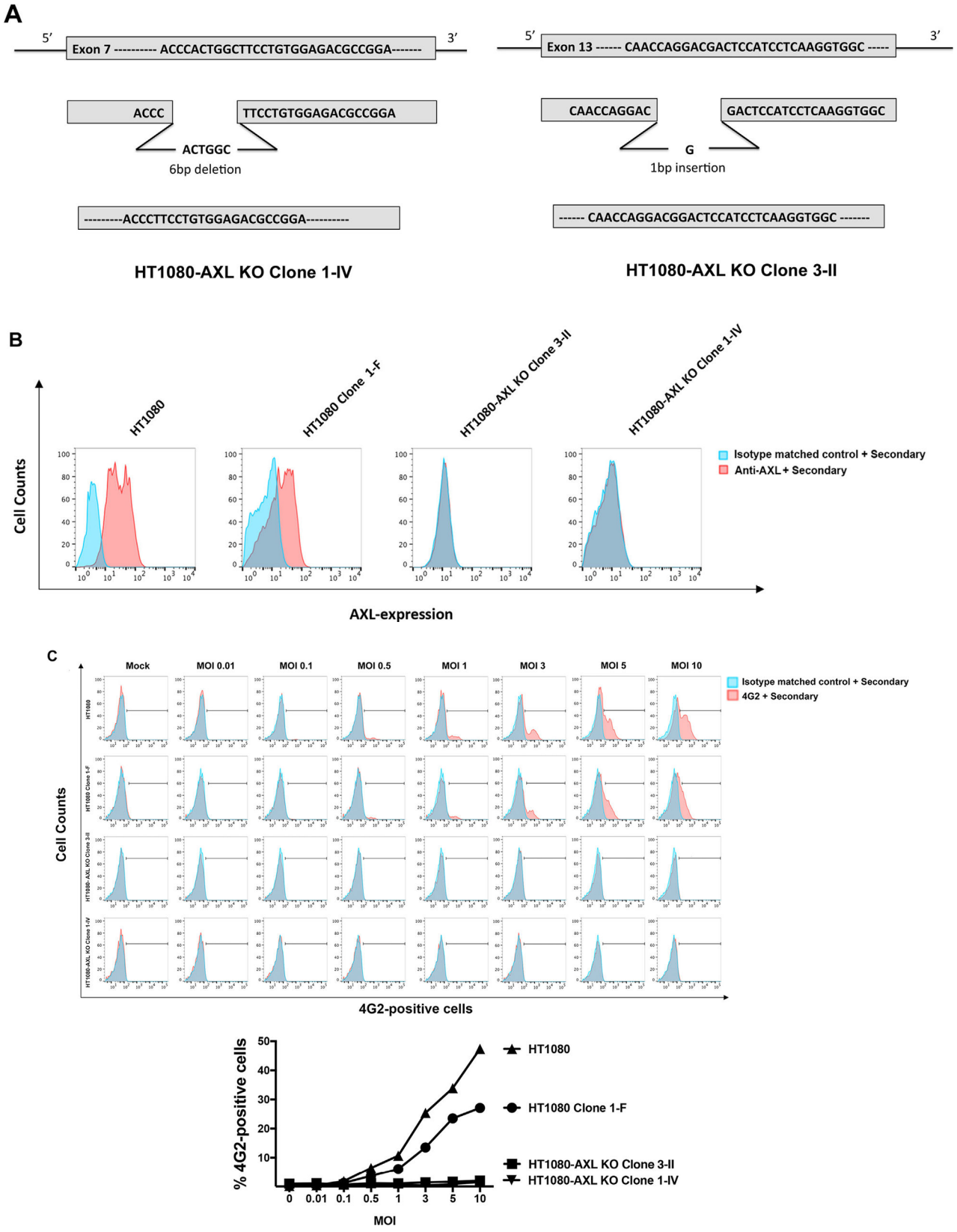

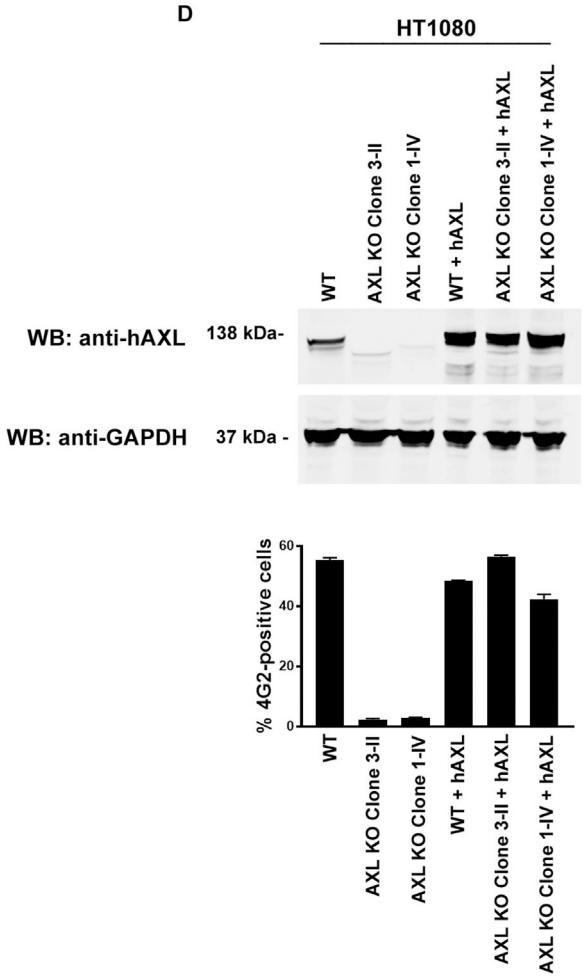

Fig. 3. Role of AXL in ZIKV infection.

(A) Construction of human HT1080 cells that do not express the AXL receptor. HT1080 cells were transiently transfected wit the CRISPR-Cas9 system using a guide RNA that targets exon 4 and 13. **(B)** Single-cell clones were analyzed for surface expression of AXL using anti-AXL antibodies by flow cytometry. HT1080-AXL-KO Clones 3-II and 1-IV were knockout for the expression of AXL. As a control, we kept the HT1080 clone 1-F, which underwent the CRISPR-Cas9 treatment but did not lose AXL expression. **(C)** HT1080 cells that do not express the AXL receptor are not infected by ZIKV-MR766. HT1080-AXL KO clones 3-II and 1-IV were challenged by ZIKV-MR766 with the indicated MOIs. Twenty-four hours post-challenge cells were fixed/permeabilized, and infection was determined by staining cells using anti- envelope antibodies 4G2. The percentage of infected cells was measured by determining the number of 4G2-positive cells using a flow cytometer (upper panel). As a control, we infected the parental and clone 1-F HT1080 cells, which express the protein AXL. A plot of the percentage of infection (% 4G2-positive cells) versus the used MOI is shown (lower panel). **(D)** Expression of human AXL (hAXL) protein on HT1080-AXL KO cells rescues the infection by ZIKVs. Expression of hAXL in HT1080-AXL KO clones transduced with the hAXL gene was tested by Western Blotting using anti-hAXL antibodies (upper panel). As a loading control, samples were also assayed for the levels of

GAPDH using anti-GAPDH antibodies (upper panel). HT1080-AXL KO transduced expressing the hAXL protein were challenged with ZIKV-MR766 using an MOI= 1. Twenty-four hours post-challenge cells were fixed/permeabilized, and infection was determined by measuring the percentage 4G2-positive cells. Experiments were repeated three times and a representative experiment with standard deviations is shown.

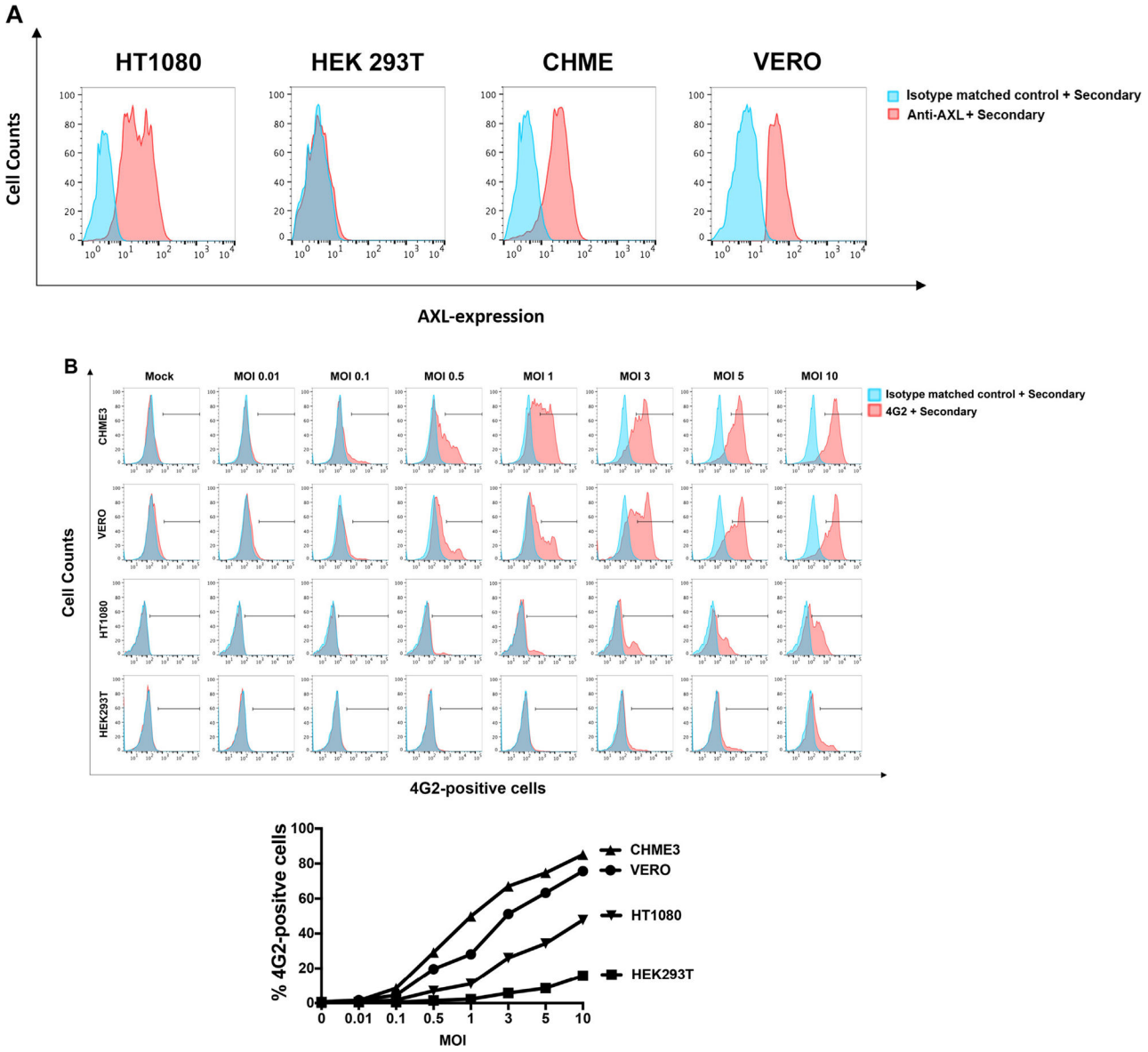

Fig. 4. Susceptibility to ZIKV infection by different cell lines correlates with AXL expression.

(A) Surface expression of human AXL of the indicated cell lines was measured in fixed cells by flow cytometry using anti-hAXL antibodies. As a control an isotype match antibody was used. Experiments were repeated at least three times and a representative experiment is shown. **(B)** The indicated cell lines were challenged by ZIKV-MR766 using increasing MOIs. Twenty-four hours post-challenge cells were fixed/permeabilized, and infection was determined by measuring the percentage 4G2-positive cells. A plot of the percentage of infection (% 4G2-positive cells) versus the used MOI is shown (lower panel). Experiments were performed at least three times and a representative experiment is shown.

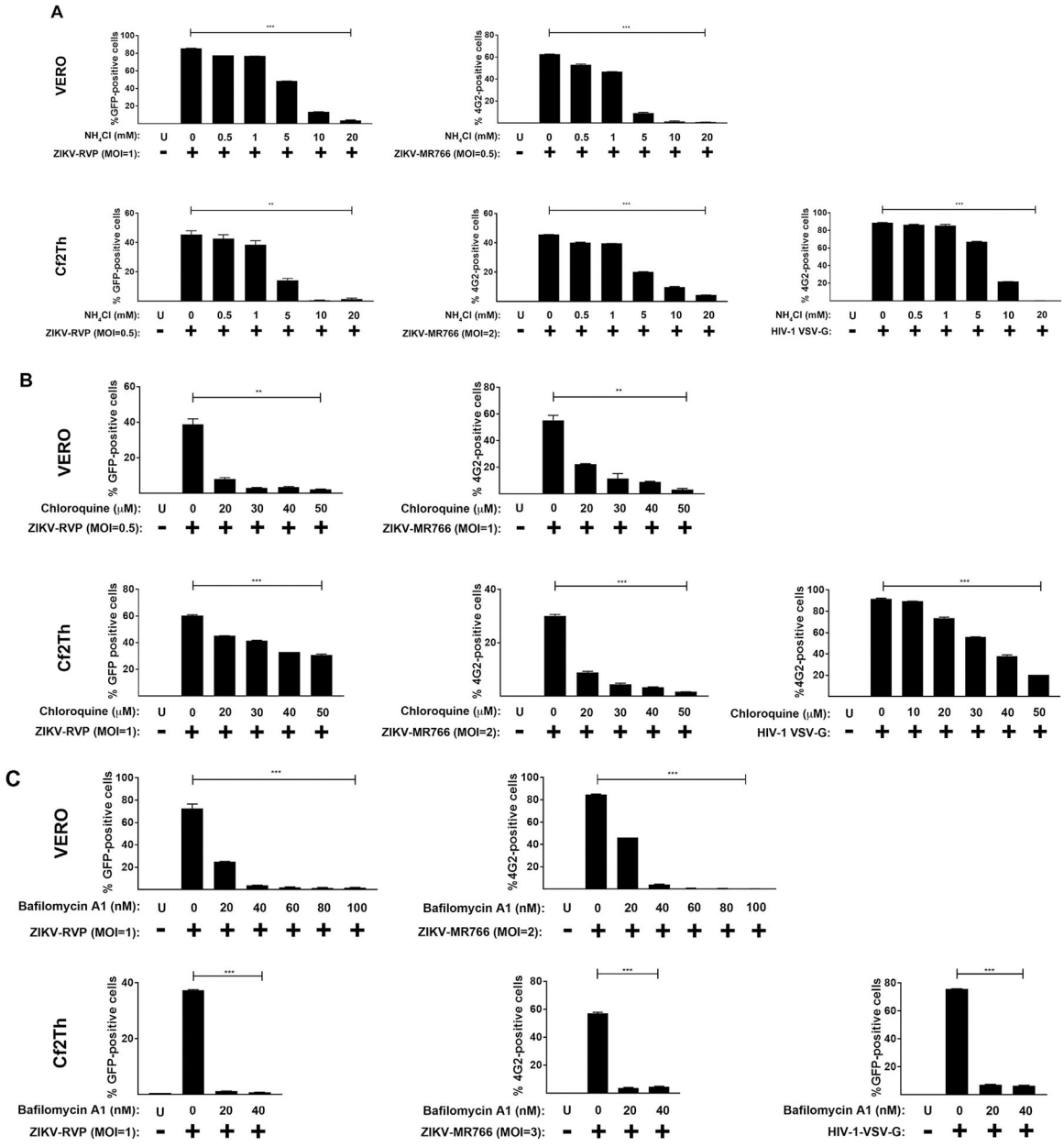

Fig. 5. Lysosomotropic agents block ZIKV infection.

Ammonium Chloride, Chloroquine and Bafilomycin A1, inhibit ZIKV infection. VERO and Cf2Th cells were challenged with ZIKV-RVPs or ZIKV-MR766 at the indicated MOI in the presence of increasing concentrations of ammonium Chloride **(A)**, Chloroquine **(B)** or Bafilomycin A1**(C)**. All drugs were used at concentrations that were not toxic to cells. Forty-eight hours post-challenge infection was determined by measuring the percentage of GFP-positive or 4G2-positive cells for ZIKV-RVPs or ZIKV-MR766 infections, respectively. As a control, similar experiments were performed using the pH-dependent pseudo-typed virus HIV-1-VSV-G. Experiments were repeated at least three times and a representative experiment is shown. $P < 0.05$ (*), $P < 0.01$ (**), $P < 0.001$ (***) or not significant (ns), using two-tailed Student's t-test are shown. U: not infected and not treated.

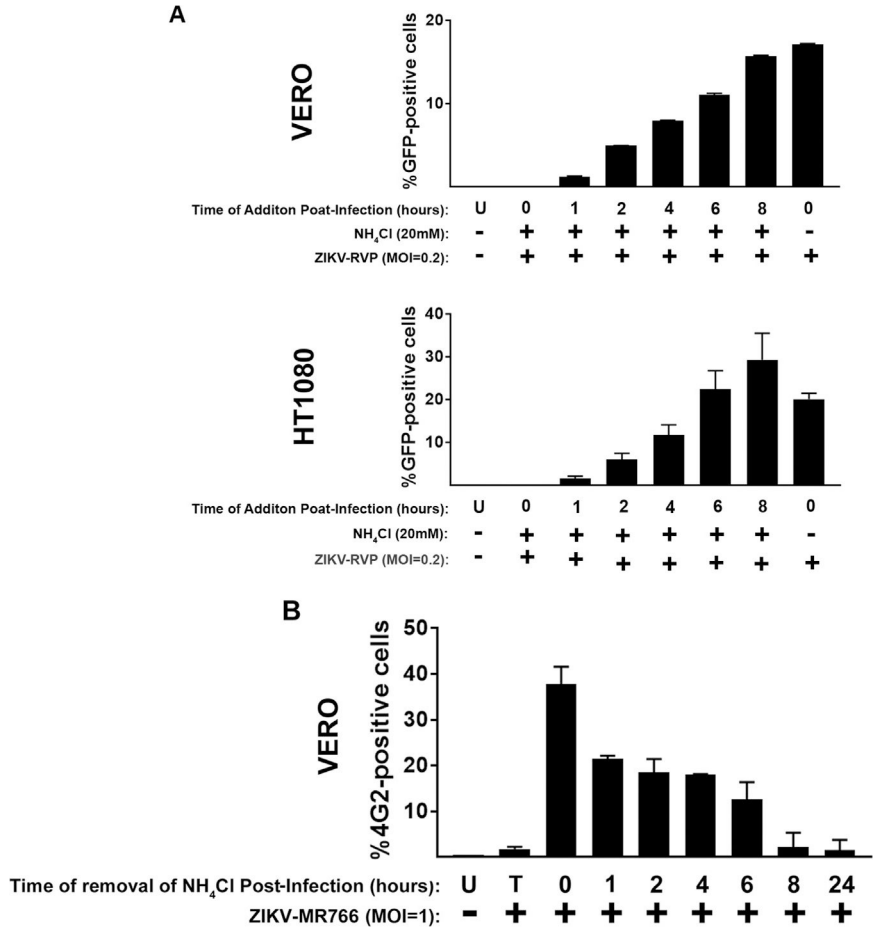

Fig. 6. ZIKV in the endocytic pathway.

(A) Kineticts of ZIKV entry. ZIKV-RVPs were pre-bound to Vero or Cf2Th cells at 4 °C for 1. Infection was initiated by shifting the temperature to 37 °C. At the indicated time points, cells were treated with 10 mM ammonium chloride to stop infection. Forty-eight hours post-challenge infection was determined by measuring the percentage of GFP-positive or 4G2-positive cells for ZIKV-RVPs or ZIKV-MR766 infections, respectively. As a control, similar experiments were performed using the pH-dependent pseudo-typed virus HIV-1-VSV-G. **(B)** Stability of ZIKVs in the endocytic compartments. ZIKV-MR766 viruses were pre-bound to Vero cells at 4 °C for 1 in the presence of 10 mM of ammonium chloride. Infection was initiated by shifting the temperature to 37 °C. At the indicated time points, ammonium chloride was removed to allow the fusion of intact viruses. Forty-eight hours post-challenge infection was determined by measuring the percentage of 4G2-positive cells. Experiments were repeated at least three times and a representative experiment is shown. U: not infected and not treated, T: infected and treated at time 0.

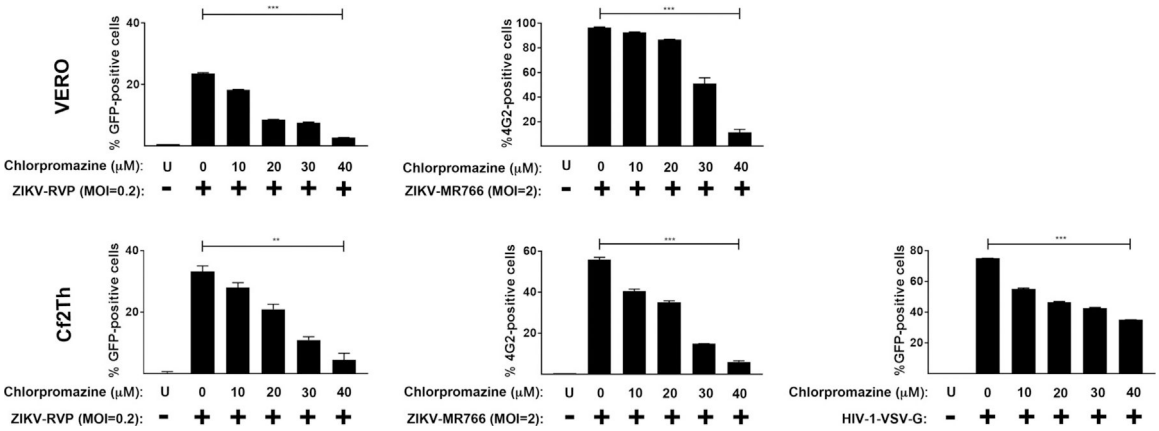

Fig. 7. Clathrin-mediated uptake is involved in the entry of ZIKVs.

ZIKV-RVPs and ZIKV-MR766 were pre-bound to Vero or Cf2Th cells at 4 °C for 1 h in the presence of increasing concentrations of chlorpromazine. Infection was initiated by shifting the temperature to 37 °C. Seven hours post-challenge the infection culture was replaced with fresh media. Forty-eight hours post-challenge infection was determined by measuring the percentage of GFP-positive or 4G2-positive cells for detection of ZIKV-RVPs or ZIKV-MR766 infection, respectively. As a control, similar experiments were performed using the pH-dependent pseudo-typed virus HIV-1-VSV-G. Experiments were repeated at least three times and a representative experiment is shown. $P < 0.05$ (*), $P < 0.01$ (**), $P < 0.001$ (***) or not significant (ns), using two-tailed Student's t-test are shown. U: not infected and not treated.